Changes in the Morphology of Bulk Spherulitic Nylon 6 Due to Plastic Deformation

A. Galeski,† A. S. Argon, and R. E. Cohen*

Massachusetts Institute of Technology, Cambridge, Massachusetts 02139.
Received November 12, 1987

ABSTRACT: The change in spherulitic morphology of bulk nylon 6 due to plastic deformation was studied by means of transmission electron microscopy of ultrathin sections. Fixation of morphology was achieved by using quick cooling and infiltration with OsO_4 before sectioning. Transmission electron microscopy of ultrathin sections cut from the neck regions of specimens deformed to draw ratios from 2 to 3 reveals spherulitic structures, although no regular lamellar structure could be detected within spherulites. The impression of the presence of spherulites is created by radial orientation of dark spots and radially arranged strips of stained material. The dark spots are small regions of nylon 6, in which the microstructure is damaged during deformation and reacts and cross-links with OsO_4. For the same strain, the number of dark spots decreases with increasing water content in the material and with decreasing crystalline fraction. Density decreases of deformed samples, as well as DSC data, indicate that the dark spots are regions of very low density, suggesting that the dark spots are cavities formed to relieve stresses due to material misfit developed between domains of lamellae and between different spherulites during the course of plastic deformation.

Introduction

The mechanical behavior of spherulitic semicrystalline polymers depends on many morphological factors, including molecular weight and its distribution; degree of crystallinity; the size, shape, and perfection of crystals; and the size of spherulites. It has been shown in nylon 6 that there is a significant increase in yield stress and modulus with increasing density and crystallinity.[1] There are many conflicting data on the influence of spherulite size on the mechanical behavior of semicrystalline polymers; this follows from the fact that spherulite size changes along with the size and perfection of lamellae[2] and the amount of intercrystalline links and tie molecules.[3,4] These parameters also affect the deformation habit, i.e., the deterioration of spherulitic structure during deformation and fracture. It has been shown for other polymers, by Hay and Keller[5] for thin spherulitic films and by Samuels[6] for relatively thicker samples, that the deformation is not uniform and depends on the orientation of lamellae inside spherulites with respect to the deformation direction. Other habits of deformation have also been observed[7,8] for various polymers, including nylon 6.[9] When the draw direction and the radius of spherulites are nearly parallel, i.e., in polar zones, the deformation has been reported to be the extension of lamellae;[6] some intraspherulitic cracks have also been found.[9] In equatorial zones, in which the deformation direction and the radius of spherulites are at right angles, the deformation is considered to take place by extension of interlamellar material. For the remaining parts of spherulites, shear of both the lamellae and interlamellar regions occurs, associated with rotations of the lamellae. Other studies indicate the importance of interspherulitic boundaries and weak spots between spherulites.[10,11]

From the work of Peterlin,[12,13] it is known that the plastic deformation of a semicrystalline polymer, such as polyethylene, eventually destroys and unravels the stacks of thin and long parallel lamellae to transform them into densely packed thin microfibrils. This transformation has been reported to be complete at a draw ratio that is between 2 and 3 in nylon 6.[12,13] Consequently, it is also believed that spherulitic order in nylon 6 must become erradicated at such a draw ratio.

In this work, we have examined changes in the morphology of nylon 6 due to plastic deformation as a function of initial morphology and water content. In particular, we focused on revealing to what extent the spherulites become altered by drawing in the neck zone and the changes the lamellae suffer as a result of drawing. New techniques for fixation of changes of morphology and sectioning of deformed samples for the purpose of transmission electron microscopy were required for this work and are described here as well.

Experimental Procedure

Samples. Polyamide 6 (Capron 8200 extracted, Allied Corp.) was used in this work. Size-exclusion chromatography using trifluoroethanol as a mobile phase revealed a weight-average molecular weight, M_w, of 32 600 g/mol and a polydispersity index, M_w/M_n, of 1.80 for Capron 8200. Plaques of 3 mm thickness were obtained by compression molding. The outer layers of the plaques were removed by machining at room temperature, leaving a 1 mm thick core for further studies. The morphology of deformed and undeformed samples of a reaction injection molded nylon 6 was also studied for comparison; this material (RIM, Monsanto Polymer Products Co.) was supplied in the form of 3 mm thick plates.[14] The RIM specimens were used without further processing, except for machining off the skin. The weight-average molecular weight of RIM nylon 6 was M_w = 40 700 g/mol and M_w/M_n = 1.83, as determined by size-exclusion chromatography.

Oar-shaped samples for tensile testing were cut from machined cores of plaques and plates. The gauge length of specimens was 19.1 mm and the width was 3.2 mm. All surfaces of the specimens were rough ground with 800 mesh silicon carbide paper and then carefully polished with 0.3-μm powder and finally with 0.05-μm powder. Care was taken to prevent heating of the specimens during all preparations. Polished tensile specimens were then dried at 100 °C in vacuum for 24 h.

Samples were divided into three groups: the first was stored in a dry atmosphere in a desiccator, the second was conditioned over a saturated water solution of calcium nitrate (60% relative humidity at room temperature) for at least 7 days, and the third group of samples was submerged in distilled water for at least 3 days prior to further studies. These conditioning histories were selected on the basis of experimental convenience and do not necessarily correspond to treatments required to bring samples to equilibrium moisture contents.

Tensile Testing. All tensile tests were performed on a Model 1122 Instron tensile testing machine. Shortly before testing, the samples were removed from the conditioning chambers, quickly mounted in Instron grips, and tested at an average strain rate of 2.6×10^{-4} s^{-1}.

Morphology Investigation. The morphology of undeformed samples was examined by means of polarizing light microscopy of thin sections and by means of transmission electron microscopy (TEM) of ultrathin sections. The procedure for ultrathin sectioning of bulk nylon 6 has been described by us elsewhere.[15]

† On leave from the Center of Molecular and Macromolecular Studies, Polish Academy of Sciences, 90-362 Lodz, Poland.

0024-9297/88/2221-2761$01.50/0

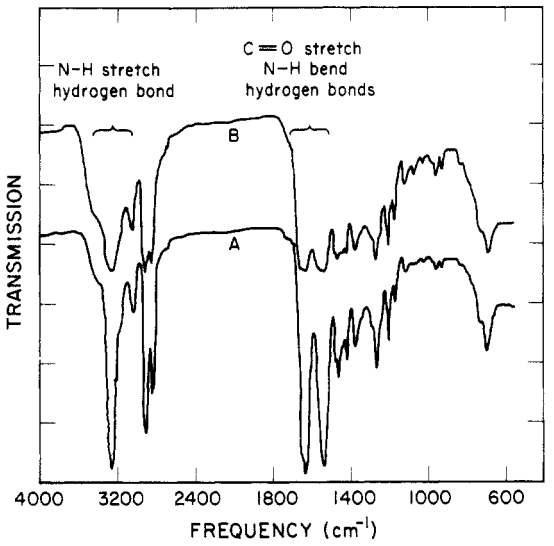

Figure 1. Infrared absorption spectra of nylon 6 film cast from trifluoroethanol: (A) melt annealed and crystallized; (B) same as (A), but treated with OsO_4.

Several potential procedures were examined for fixation of morphology of bulk nylon 6 samples following deformation to preserve the as-deformed structure for detailed study. These are as follows: treatment with glutaraldehyde; cross-linking with phosphotungstic acid; cross-linking with phosphotungstic acid and a small amount of benzyl alcohol for promoting diffusion; cross-linking with phosphotungstic acid and glutaraldehyde with a small amount of benzyl alcohol; treatment with vapors of osmium tetroxide; infiltration with osmium tetroxide solution in water; infiltration with osmium tetroxide with a small amount of trifluoroethanol in water and rapid drop in temperature. Out of these procedures, the best method for fixation of changes in the morphology was found to be the combination of rapid drop in temperature and infiltration with osmium tetroxide in the following way: Immediately after reaching the required state of deformation, the sample is quickly submerged in 1–2 wt % water solution of OsO_4 at a temperature from 0 to 5 °C and held for several days. The addition of trifluoroethanol (1–2 wt %) promotes the infiltration of samples with OsO_4 and significantly reduced the time required for full penetration. Finally, the temperature is slowly raised to room temperature, accelerating the chemical reaction between OsO_4 and deformation-damaged nylon 6 molecules.

In undeformed Capron, OsO_4 slowly attacks C=O and N—H bonds, as is clearly seen in Figure 1 from the lowering of the intensity of the 1550- and 1650-cm^{-1} bands in the IR spectra. However, it does not cause the cross-linking of undeformed Capron material; osmium-treated samples are still soluble in trifluoroethanol and other solvents. In contrast, undeformed RIM nylon 6 becomes cross-linked, probably due to the different chemical nature of chain ends, as compared to Capron. Damage done to the chemical structure of nylon 6 macromolecules during machining, polishing, or cutting causes the strong chemical cross-linking with OsO_4. Surfaces produced by molding are not cross-linked by osmium tetroxide. It follows then that only those changes in Capron nylon 6 morphology which are accompanied by chain rupture can be preserved by treatment with OsO_4; other changes such as reversible deformation or plastic deformation without chain rupture are not fixed by the technique employed here.

Tensile samples were prepared from injection molded Capron 8200 and conditioned at 60% relative humidity prior to deformation. To evaluate the effectiveness of the OsO_4 fixing procedure, one specimen was submerged for 8 days in a 1 wt % water solution of OsO_4, while another was kept for 8 days in distilled water, both in a stressed state at 4 °C. The specimens were slowly heated up to room temperature and then removed from the baths, and the residual liquids were wiped off. Upon release of the stress, a sudden retraction of the length of both specimens was observed, as shown in Figure 2, which can be attributed to elastic response.

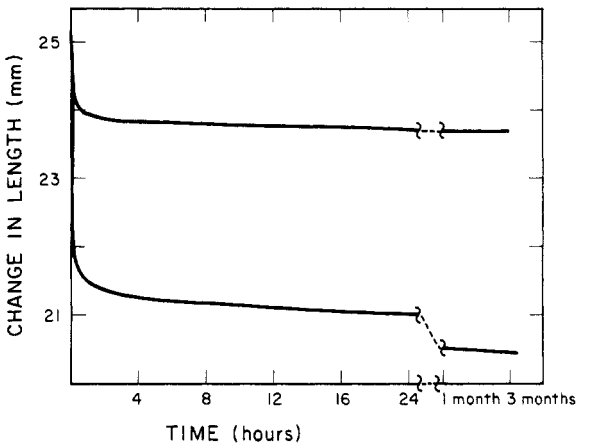

Figure 2. Changes in the length of tensile specimens, taken to a strain of 0.32, after release of stress. Top curve, sample cooled to 4 °C and infiltrated with OsO_4 for 8 days under stress; lower curve, sample cooled to 4 °C and soaked in distilled water for 8 days under stress.

After this, the length of the specimen treated with OsO_4 did not change significantly with time, while continuous slow shrinkage of the other specimen was observed. The difference in changes of the length becomes even more pronounced at elevated temperature, indicating that in the material treated with OsO_4 after deformation, most of the time-dependent recovery processes are frozen, and the corresponding deformation-induced changes in morphology are fixed by cross-linking with OsO_4.

Small filaments of about 100 μm × 100 μm in cross-section and a few millimeters in length were cut from different regions of the deformed tensile specimens after fixation with osmium tetroxide. The filaments were embedded in a mixture of epoxy and phenolic resins following the procedure described previously by us[15] for undeformed nylon 6 samples. The specimens were sectioned by means of a LKB Cryo-Ultratome V at −30 °C. Ultrathin sections were collected on a mixture of dimethyl sulfoxide and water. Sections were straightened out by floating them on the surface of distilled water at room temperature. The sections were then stained with phosphotungstic acid for 20 min. The sectioning and staining procedures are described by us in detail elsewhere.[15]

The sections were examined by TEM using Phillips 200 and Phillips 300 microscopes operating at accelerating voltages of 80 and 100 kV, respectively. Stereomicrographs were also taken by tilting the specimen grids in the microscope ±6° from the horizontal position.

Differential Scanning Calorimetry. A Perkin-Elmer DSC IV was used for studying the melting of undeformed and deformed nylon 6 specimens. The scaning rate was 20 °C/min.

Density Measurements. Densities were measured by means of a density gradient column. The 1 m high column, covering the range from 1.00 to 1.20 g/cm^3, was filled with a mixture of toluene and carbon tetrachloride. All measurements were performed at 22 °C. The readout of the positions of the samples in the column was taken 15 min after introducing the samples.

Experimental Results

Structural Features. All samples exhibit a spherulitic morphology in which spherulites fill the entire volume. Morphological features of the undeformed nylon 6 spherulites were studied previously by us in detail by means of TEM of ultrathin sections;[15] recently, similar findings were reported by Schaper et al.[16] The undeformed spherulites are composed of long flat (untwisted) ribbon-like lamellae, having a thickness of 50–60 Å, a width of 150–600 Å, and a length, parallel to the radial direction, that could be as long as the distance between the point of origin to the spherulite boundary. The length was often of the order of several micrometers. Three or four neighboring lamellae are usually parallel to each other and form domains as a result of low-angle noncrystallographic branching of lamellae during crystallization. The domains

Table I
Density and DSC Data for Nylon 6 Undeformed and Deformed Samples

	dried	60% rel humidity	water soaked
	Compression Molded Capron		
undeformed density, g/cm³	1.1295	1.1390	1.1380
deformed density, g/cm³	1.0875	1.1160	1.1390
undeformed enthalpy of melting, J/g/peak temp	54.9/226 °C	61.4/225 °C	57.5/224 °C, additnl peak at 21 °C
deformed enthalpy of melting, J/g/peak temp	57.2/223 °C	58.6/221 °C	67.6/223 °C
water content	500–800 ppm	3.3 ± 0.1 wt %	7.0 ± 0.2 wt %
	Injection Molded Capron		
undeformed density, g/cm³	1.1270	1.1340	1.1350
deformed density, g/cm³	1.1085	1.1225	1.1390
undeformed enthalpy of melting, J/g/peak temp	64.4/223 °C	66.5/222 °C	59.4/224 °C
deformed enthalpy of melting, J/g/peak temp	64.0/223 °C	64.3/223 °C	65.4/223 °C
water content	500–800 ppm	3.3 ± 0.1 wt %	7.0 ± 0.2 wt %

of lamellae radiate from the centers of spherulities, with random orientation in the tangential direction. Polarizing light microscopy of thin sections cut at various angles with respect to the injection or compression direction does not show any preferential orientation of the spherulitic morphology of the cores of injection, compressionn, or reaction injection molded samples of nylon 6. Nor does the X-ray diffraction show preferred orientation of crystals.

There are two polymorphic forms present in different amounts in nylon 6 samples. Of these, the α form is more dense (1.23 g/cm³ [17]) and more stable, while the γ form is less dense (1.17 g/cm³ [17]) and less stable, but also forms lamellae. The α and γ forms differ in the position of hydrogen bonding and in the twist of the chain around amide groups. Preliminary X-ray diffraction intensities for the samples studied in this work have been presented previously,[15] revealing that in qualitative terms, the largest amount of α phase is present in RIM nylon 6, and less in the injection and compression molded Capron samples. More extensive X-ray diffraction on dry samples revealed crystallinity levels of about 25% α, and 13% γ in compression molded samples and 15% α, 28% γ in injection molded samples. Conditioning of the samples in an atmosphere of 60% relative humidity slightly increases the crystalline fraction of α and γ phases. This is also seen from the density increase, as is shown in Table I. This effect is believed to be due to plasticizing action of absorbed water in the amorphous phase (see Table I for the data on water content). Further increases of the amount of absorbed water, however, produce smaller increases in the density. The heat of melting of the samples as measured by DSC, also reported in Table I, slightly depends on the contitioning of the material. The trend is similar to that of the density. For samples soaked in water, a second low-temperature melting peak at 208–210 °C appears in both compression and injection molded samples.

Stress–Strain Experiments. The stress–strain (load-extension) curves for compression molded samples are depicted in Figure 3. Each curve represents a mean, obtained from testing at least three samples. Compression

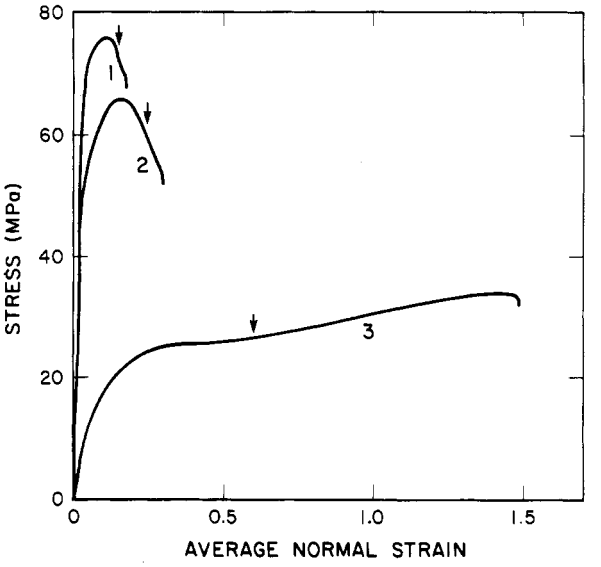

Figure 3. Stress–strain curves for compression molded nylon 6 samples: (1) dried at 100°C for 24 h in vacuum; (2) conditioned at 60% relative humidity; (3) soaked in water.

molded nylon 6, when tested in a dry state, yields at 76 MPa. During yielding, a small neck is formed with a natural draw ratio of 2.16, as determined from the reduction of the cross-sectional area assuming constant volume. The neck does not propagate; instead, fracture occurs upon the formation of the neck at an engineering strain of 0.2. The compression molded nylon 6 conditioned at 60% relative humidity also shows yielding, but at a lower level of 65 MPa. Here, the strain in the neck corresponds to a natural draw ratio of about 2.25. Fracture of these samples also occurs upon formation of the neck at an engineering strain of 0.3. Samples soaked in water undergo a dramatic change in tensile behavior. A neck is formed, and the deformation homogeneously spreads over the entire gauge length of the samples. Yield occurs at 25 MPa, followed by neck extension and mild strain hardening. Fracture occurs at a normalized elongational strain of 1.5 and after reaching a flow stress of 33 MPa. The natural draw ratio was found to be 2.50 for these water-soaked samples.

The stress–strain (load-extension) curves for injection molded Capron are presented in Figure 4. Injection molded samples in the dry state yield at a stress of 72 MPa and fracture almost immediately after formation of a neck. A small amount of absorbed water in these samples after conditioning at 60% relative humidity causes a drastic softening, decreasing the yield stress to 43 MPa; these samples stretch quasi-homogeneously and show some strain hardening. Fracture occurs at a nominal strain of 1.2 at a stress of 45 MPa. The natural draw ratio is about 2.6. Soaking in water reduces the yield stress further to 20–23 MPa, where the samples now exhibit quite homogeneous drawing without necking. The natural draw ratio, as measured from the change in the cross-sectional dimensions, is 2.7.

The densities of deformed samples at strain levels marked by arrows in Figures 3 and 4 are presented in Table I. The natural draw ratios of the portions of the material taken for the density measurements were between 2.1 and 2.7, while the engineering strains are very different, depending on how much of the gauge length is stretched before fracture occurs. The portions of the material for the density measurement were always cut from the interior of the sample in the middle of the neck or gauge length. The density of dry nylon 6 samples prepared from com-

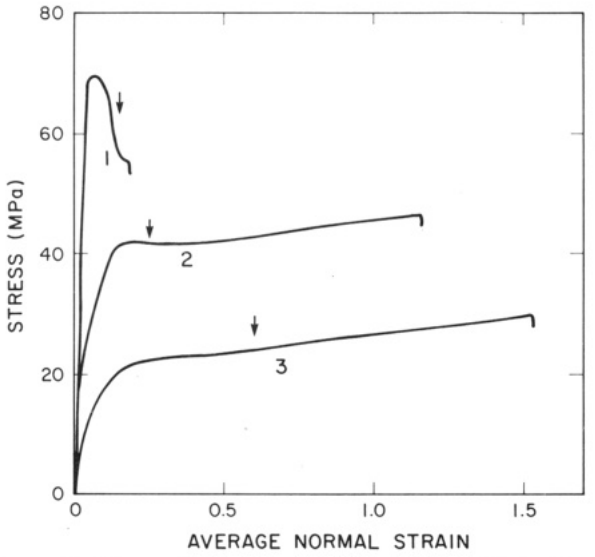

Figure 4. Stress–strain curves for injection molded nylon 6 samples: (1) dried at 100°C for 24 h in vacuum; (2) conditioned at 60% relative humidity; (3) soaked in water.

pression molded plaques is reduced by deformation almost to the level of the amorphous material (1.078 g/cm^3[17]). In the case of injection molded material, the density of dried and subsequently deformed samples is also low, but not as low as for compression molded material. The pieces of the material cut from the neck region, but near the surface, show much less drop in the density (to 1.1135 and 1.1025 g/cm^3 for injection and compression molded samples, respectively), indicating the important role of negative pressure present in the center of the neck in the density reduction there. The presence of water in the material in small amounts reduces the amount of density decrease caused by deformation, no doubt, due to the lowered level of plastic resistance in these materials. Samples conditioned initially by soaking in water slightly increase their density during deformation.

DSC measurements were also carried out on the deformed samples for comparison with the density measurements. In all deformed samples, there is only one melting peak, appearing in the temperature range 221–224 °C, which indicates that some recrystallization takes place during deformation of soaked samples. The heat absorbed during melting of deformed samples is only slightly different from that of undeformed samples. In the case of deformed samples of nylon 6 soaked in water, there is an increase in the heat of melting with respect to undeformed samples, furnishing further support for an increased level of deformation induced crystallinity in these materials compared to the dried material. The discordant results of a relatively high level of crystallinity, as determined from DSC measurements, and the low density of deformed samples (dried and conditioned at 60% relative humidity) suggest that the drawing does not reduce the crystallinity, but produces voids, or at least regions of very low density within the material. Examination of the morphologies of the deformed samples was undertaken to verify or refute this postulate.

Transmission Electron Microscopy. Transmission electron microscopy was carried out on ultrathin sections of material which had been fixed prior to sectioning. To provide a feel for the nature of the fixing process, the slightly magnified views of deformed samples are shown in Figure 5, revealing the results of the fixing process on longitudinal sections of 0.2 mm thickness of three compression molded Capron samples dried and then deformed

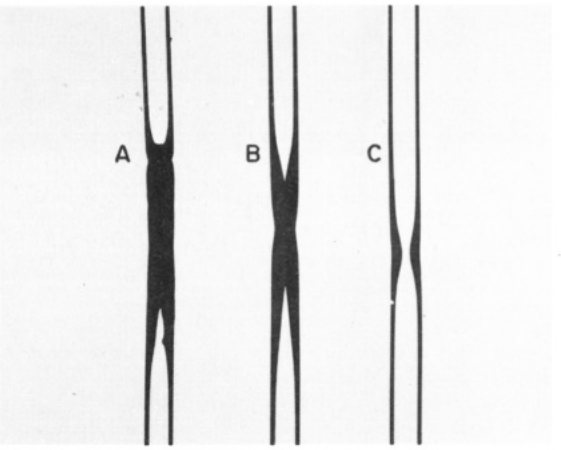

Figure 5. Longitudinal sections of compression molded dry nylon 6 samples deformed to a strain of 0.15: (A) deformed and immediately cooled to 4 °C and infiltrated for 7 days with OsO_4 under stress; (B) deformed and relaxed under strain for 24 h at room temperature, then treated as sample A; (C) deformed and stress released and then treated as sample A.

to an engineering strain of 0.15. Sample A was cooled to 4 °C immediately after deformation, and infiltrated for 7 days with OsO_4 under stress; sample B was held at fixed length and allowed to undergo stress relaxation for 24 h before cooling and infiltration with OsO_4; sample C was removed from the grips, cooled to 4 °C, and infiltrated with OsO_4 in the absence of external stress. The dark regions in Figure 5 show the range of penetration of OsO_4, and its subsequent reduction to osmium dioxide or osmate ester.[18] It is seen that the range of penetration is largest in sample A with fixed ends cooled immediately after deformation and infiltrated with OsO_4, smaller in sample B with fixed ends, but allowed to undergo stress relaxation at room temperature, and smallest in sample C, with free ends, where penetration of OsO_4 has not even reached the center of the sample. It appears that the deformation of nylon 6 opens paths of fast diffusion, and the applied stress keeps them open; stress relaxation and unloading at room temperature apparently promote some healing and close up the fast diffusion paths. Thus, in order to retain the morphological change that results from the deformation, the fixation of all deformed samples for the purpose of TEM morphology studies was performed on stressed samples with their ends held in jigs.

The OsO_4 infiltration under stress for the deformed samples which were conditioned at 60% relative humidity and soaked in water does not reveal such intense penetration of OsO_4, as in the case of dried and subsequently deformed samples. Apparently, fewer fast diffusion paths are created in these samples during deformation.

Parts a and b of Figure 6 show electron micrographs of ultrathin sections of undeformed Nylon 6 samples prepared from compression molded and injection molded plaques, respectively. The samples were subjected to infiltration with OsO_4 prior to sectioning; however, OsO_4 treatment alone does not sufficiently enhance the contrast between crystalline and amorphous phases of nylon 6, and therefore, the sections were also stained with phosphotungstic acid.[15,16,19] Spherulitic structure is clearly seen in both micrographs. Higher magnification micrographs reveal well-defined lamellae arranged in domains within spherulites, indicating that the OsO_4 treatment does not disturb lamellar and spherulitic arrangements in nylon 6. No difference was observed in ultrastructure between conditioned and dried samples in the undeformed state.

Figure 7a–d shows electron micrographs of transverse ultrathin sections of deformed dried and conditioned nylon

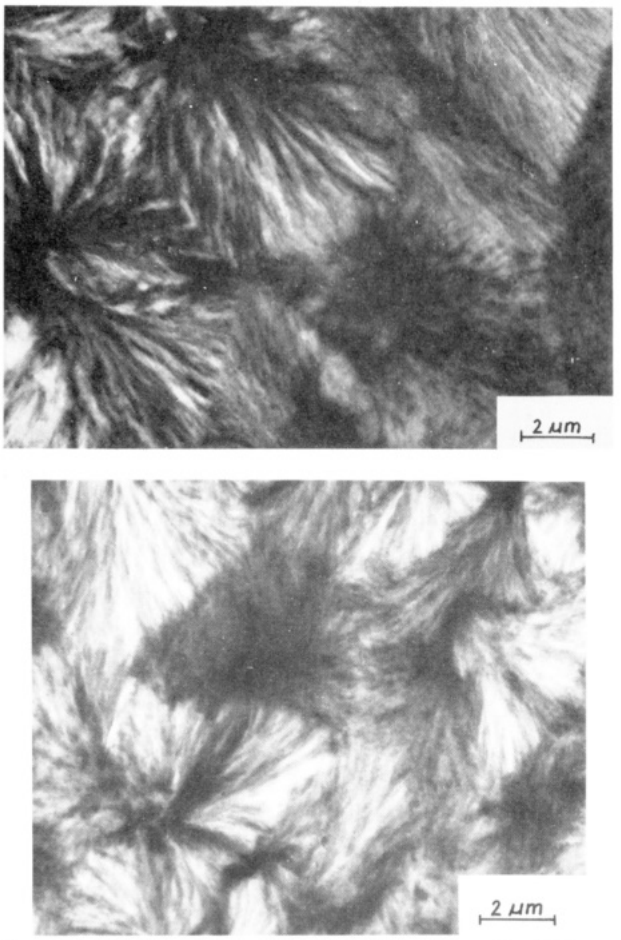

Figure 6. Electron micrograph of ultrathin section of undeformed samples of nylon 6, infiltrated with OsO_4, and stained with phosphotungstic acid after sectioning: (a, top) compression molded Capron; (b, bottom) injection molded Capron.

6 samples. The arrows in Figures 3 and 4 indicate the levels of strain of the samples from which Figure 7a–d was obtained. In these micrographs, it is still possible to distinguish the outlines of spherulites. In parts a and b of Figure 8, the electron micrographs of longitudinal ultra thin sections of deformed dried and OsO_4 treated and untreated RIM nylon 6 samples are presented, respectively. The knife edge was parallel to the drawing direction during cutting. The sections were subsequently stained in PTA. In these sections, the outlines of elongated spherulites can also be resolved. Phosphotungstic acid staining reveals some radially arranged spotty strips of higher staining susceptibility, which create the image of spherulites; however, there is a drastic change in the appearance of ultrastructure due to deformation. The lamellae can no longer be distinguished in any of the deformed samples. In the dried samples and those conditioned at 60% relative humidity, there is a dense population of dark features, which are seen in sections with or without phosphotungstic acid staining. The dark spots are seen in those parts of sections which are cut across or close to the centers of spherulities, i.e., in their equatorial regions with respect to the deformation direction. They are arranged along spherulite radii. No dark spots were found in the polar regions of spherulites, defined with respect to the deformation direction. It is also seen that the centers of spherulites are relatively free from dark spots, and that their largest concentration is found in regions where three spherulites meet.

Figure 9 shows a stereopair of electron micrographs of the ultrathin section of the deformed, dried, compression molded sample. The dark spots which form along the spherulite radius have elongated shapes with aspect ratio of about 2–3. In the samples conditioned at 60% relative humidity, there are fewer of these dark spots, particularly in the injection molded samples. Ultrathin sections of water-soaked samples reveal only very few dark spots, and they are much smaller than in either the deformed dried samples and 60% relative humidity conditioned samples.

Figure 10 shows an electron micrograph of an ultrathin section of the deformed, dried, injection molded sample. This sample was not treated with OsO_4 before embedding and sectioning. No dark spots similar to those observed in the OsO_4 treated samples are seen in Figure 10. Therefore, it becomes evident that OsO_4 makes it possible to observe the damage zones of deformed nylon 6 samples.

Figure 11 shows an electron micrograph of an ultrathin section of the deformed RIM nylon 6 sample conditioned at 60% relative humidity. Similar dark features are also identified in this type of nylon 6 and in quantities much higher than the corresponding Capron sample. The deformed, dried RIM nylon 6 contains even more dark spots after fixation with OsO_4. It is generally apparent that the larger crystalline fractions and/or stiffer and less water plasticized amorphous phase leads to increased amounts of dark spots in the deformed nylon 6 samples.

The deformed samples, after fixation with OsO_4, are still soluble in solvents for nylon 6, including trifluoroethanol; however, the surface layer of each sample, deformed or undeformed, is insoluble and can be removed. The remaining solution is bluish. Centrifiguration of this solution at 10000*g* for 20 min settles a black sediment, and the solution above becomes clear. Much more sediment was collected from dried samples than from samples containing some amount of water. The sediment was rinsed with trifluoroethanol, resuspended, and centrifugated again. The final sediment was deposited on a carbon film of an electron microscope grid and examined in the TEM. A micrograph of the deposited sediment is presented in Figure 12. The dark features of this micrograph are the dark spots seen in the previous micrographs of the ultrathin sections of deformed samples of nylon 6. Examination of these thinner specimens better resolves the morphology of the dark spots; they are composed of a few (usually two or four) parallel dark rods having a length from 300 to 700 Å. Since they were deposited on the carbon film at random, they can be seen in various projections, sides, or ends facing the grid. Around each group of dark rods, there is a layer of insoluble nylon 6 from 100 to 400 Å thick.

The material comprising the dark spots seen in ultrathin sections of deformed nylon 6 samples and in deposits from trifluoroethanol are insoluble, which means that nylon 6 in those regions became chemically cross-linked by osmium tetroxide treatment. The undeformed material does not get cross-linked by osmium tetroxide. It follows that the local plastic deformation process introduces chemical changes in nylon 6 in those particular zones, which later appear as dark spots in the micrographs. Apparently, the deformation-induced internal stresses between certain parts of the spherulites exceed limits for the cavitation strength of the material in these regions. It has been known for some time that the drawing of polymers can produce free radicals (for nylon 6 see ref 20), which may result from chain rupture. Based on the results of the present work, it seems that for the levels of strain studied here, such processes are very localized in parts of the spherulites and result in the dark spots seen in the micrographs presented here, where apparently, the defor-

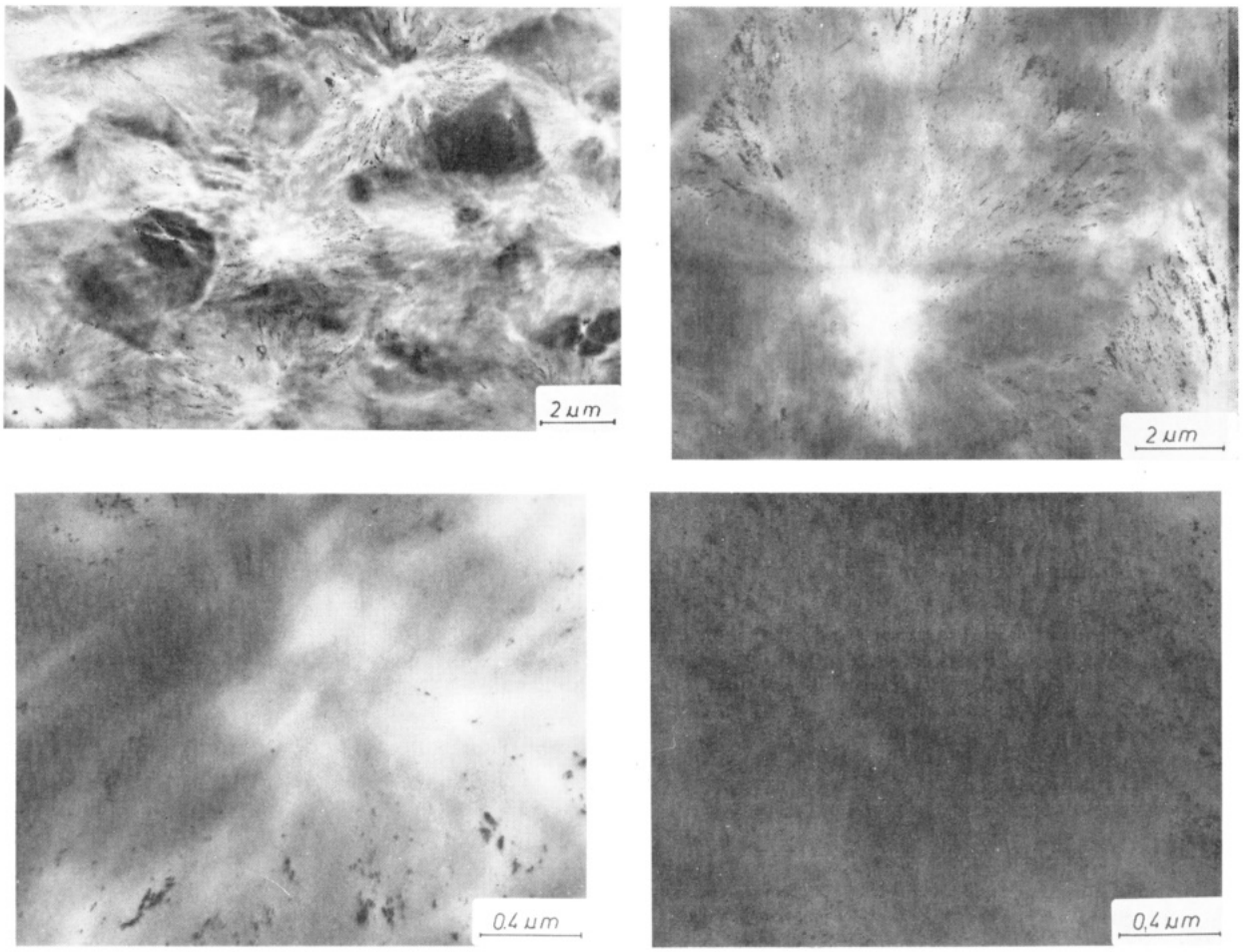

Figure 7. Transverse sections of deformed nylon 6 Capron samples: (a, top left) compression molded, dry; (b, top right) injection molded, dry; (c, bottom left) injection molded, conditioned at 60% relative humidity; (d, bottom right) compression molded, soaked in water.

mation-enhanced cross-linking of nylon surrounds actual cavities.

Removal of reduced osmium is possible by reaction with sodium metaperiodate, as was shown in the case of "black" crazes in OsO_4 treated polystyrene.[18] The electron micrograph of an OsO_4 stained section of deformed dried compression molded nylon sample, subjected to sodium metaperiodate treatment for a few hours, is shown in Figure 13. Here, white spots are seen in places where previously dark spots must have existed. The background is now darker because of phosphotungstic acid staining.

Discussion

The experimental evidence suggests that the dark spots seen in electron micrographs of deformed samples represent regions of less dense packing of the material. The likelihood that some chemical change also takes place in these regions was supported by osmium tetroxide fixation, which indicated that some chain rupture must have occurred. The combination of less dense packing of the material and some chain rupture is characteristic of crazes in amorphous polymers.[21-23] Although in many respects the rows of cavities delineated by the OsO_4 staining in the deformed samples act collectively like crazes, their irregular distribution and the semicrystalline nature of the material suggest a different mechanism of formation.

The dark spots are concentrated in equatorial zones of spherulites. Apparently, their formation results from a different mode of straining in these regions. It is known from previous work (e.g., ref 5, 6), that deformation in a spherulitic polymer is nonuniform; i.e., while the 45° inclined fans of the spherulites deform readily, the equatorial and polar fans act as plastic inhomogeneities. In addition to the equatorial fans, the dark spots are also concentrated near spherulite borders and close contact points of three sherulites, as is seen in many ultrathin sections of deformed samples. These regions of concentrated cavitation are also found in the vicinity of equatorial zones of spherulites. Since the deformation of spherulites is nonuniform, deformation misfit between regions of different effective plastic resistance readily develops inside spherulites during deformation. This gives rise to local stress concentrations of a range equal to the size of the plastic inhomogeneities, i.e., lamellae and packets of lamellae.

Although the formation of internal stresses due to inhomogeneous deformation of parts of spherulites must be quite complex, the observed zones of isolated cavities suggest certain possibilities. Figure 14 shows a possible sequence of processes. Under the imposed uniaxial tension, the packets of lamellae in the 45° fans experience resolved shear stresses that promote chain slip in the lamellae and shear in the interlamellar amorphous regions, as depicted in Figure 14a. Such inelastic deformation by simple shear in these regions is accompanied by lattice rotations, which accentuate the stresses acting on both the circular equatorial plates of the deforming spherulites, as well as on the polar regions. The primary effect of these lattice rotations is to produce tensile stresses across the faces of the equatorial plates and compressive stresses across the faces of the polar fans, as shown in Figure 14b. In addition to these, the overall elongation of the spherulites will evoke radial pressures on the equatorial plates

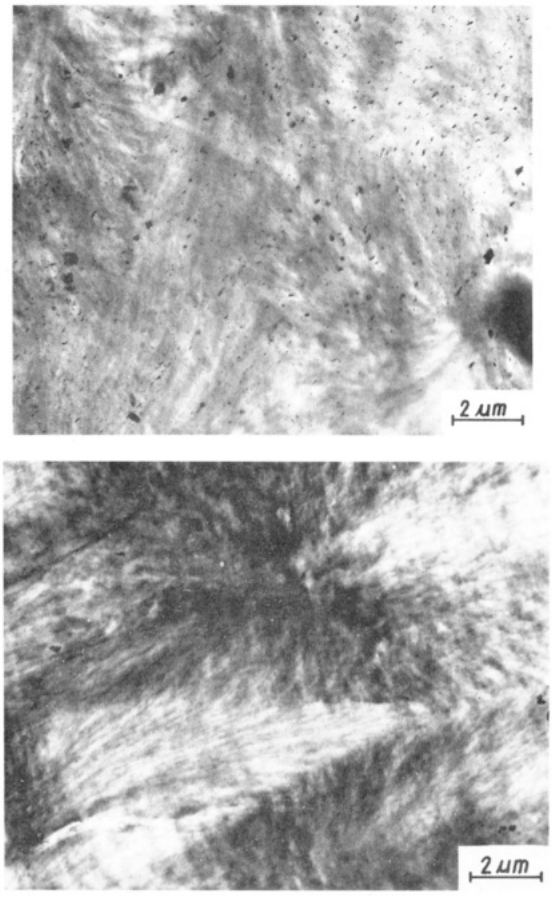

Figure 8. Longitudinal sections of RIM nylon 6 samples from specimen drawn to an extension ratio of 2: (a, top) treated with OsO_4, showing cavities with OsO_4 precipitates; (b, bottom) not treated with OsO_4, showing extended spherultes.

and additional tensile stresses in the radial direction on the polar fans, also depicted in Figure 14b. Since these accentuated stresses acting on the disks of equatorial lamellae packets have no important resolved shear components either on the interlamellar amorphous layers or on the planes of the lamellae that can promote chain slip, other more damaging types of local plastic deformation are enforced. In the equatorial disks, the stiffer radial lamellae packets act as reinforcing ribbons in the more compliant amorphous interlamellar "matrix". As is well-known,[24] compression of such composite stacks along their "fiber" axis gives rise to an unstable kinking of the fiber stacks in the interlamellar region, as depicted in Figure 14c. This produces periodic fractures in the lamellar ribbons. The accentuated tensile stresses acting across the equatorial disks then expand these periodic cracks into pores. A similar and complementary set of processes are expected to occur in the polar fans. Here, no action is expected to come from the amorphous regions, but instead, from the lamellar ribbons. In this case, the chain fold planes in the lamellae, normal to the radial direction, form an unstable stack in tension. The lamellae extend by a set of periodic kinks, as depicted in Figure 14d. Any local fractures that occur among such an inhomogeneous array of kinks would, however, be filled up by amorphous matter under transverse pressure induced by the lattice rotations, depicted in Figure 14a,b. Thus, the end result should be the arrays of aligned cavities in the equatorial disks. In samples that have been plasticized by water, the periodic kinking can be accommodated in quasi-equilibrium without resulting in fractures, hence fewer cavities.

Weak spots[11] are often found in the vicinity of contact points of several spherulites. These are formed during crystallization of bulk samples when four or more growing spherulites impinge on each other and trap a still molten pocket of material. In these weak spots, the shrinkage of the encapsulated pocket of material due to crystallization results in frozen negative pressures or, in some cases, even cavitation of the entrapped pocket, resulting in voids as large as several micrometers in size.[25] It is impossible to recognize from a single section, where such weak spots are located. For this, it is necessary to know the positions of centers of surrounding spherulites and their sizes. However, as revealed in computer simulations of crystallization,[11] at approximately 20% of all contact points of

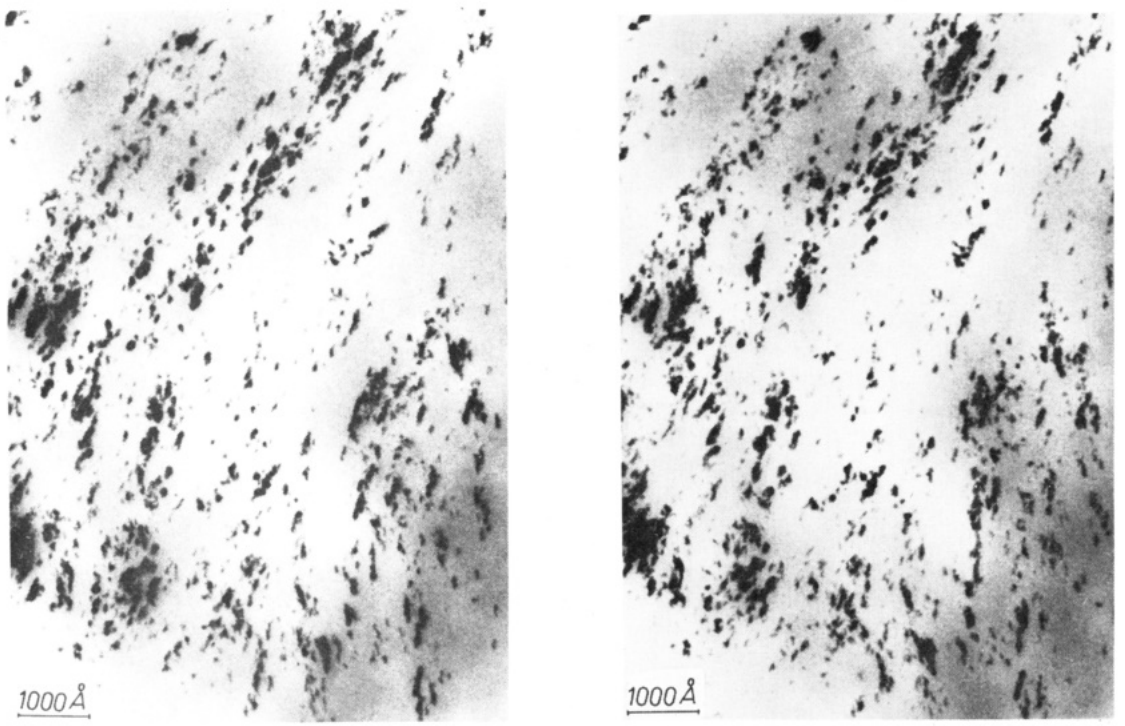

Figure 9. Stereopair of electron micrographs of ultrathin section of deformed dried compression molded nylon 6.

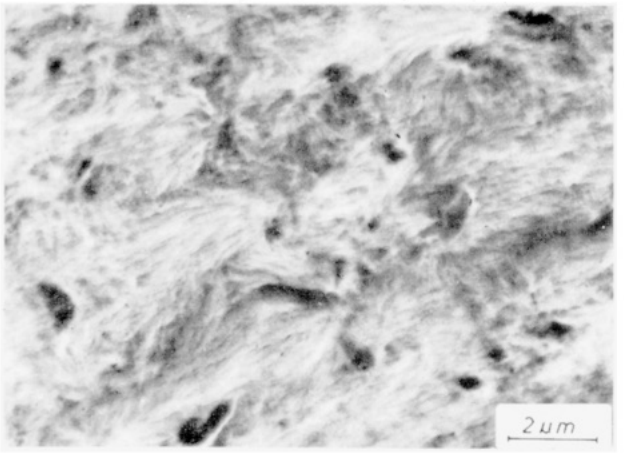

Figure 10. Electron micrograph of ultrathin section of deformed dried injection molded nylon 6, not subjected to OsO_4 treatment.

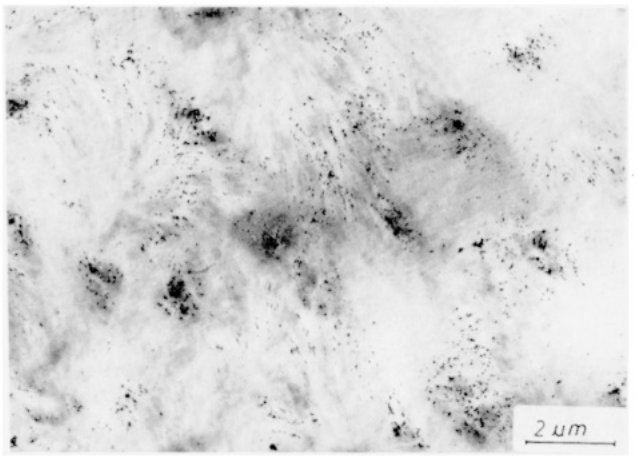

Figure 11. Electron micrograph of ultrathin section of deformed conditioned (60% relative humidity) RIM nylon 6.

spherulites these weak spots are formed. The stress applied to the sample during deformation is superimposed on the existing negative pressures in the weak spots. This may explain the concentration of dark spots around some contact points of spherulites in ultrathin sections.

Other intriguing features of dark spots are their small sizes and their orientation along spherulite radii. The dark spots seen in the sediments centrifuged from the dissolved deformed OsO_4 fixed samples have sizes of 400–600 Å, and they are split in 2–4 closely aligned thin rods of ca. 80–100-Å diameter. The overall size of the dark spots and the number of rods in a single spot suggest their close relation to the domains of parallel lamellae in undeformed sherulites, in particular to the thickness of domains (400–600 Å) and the number of lamellae (two to four) in a single domain (see ref 15). Since the domains are organized into a layered structure with alternating crystalline and amorphous phases, they are mechanically anisotropic in the directions parallel and perpendicular to the lamellar surface. Hence, the strain suffered by each domain depends on its orientation with respect to the applied stress. Because the lamellae are oriented randomly along the radii of spherulites, deformation induced between neighboring domains leads to additional strains in various directions. Local cavitation and/or chemical damage may occur if misfit related stresses exceed the cohesive strength of the material, most likely in places where already some defects exist in the structure. Noncrystallographic branching, from which new lamellae originate in undeformed material, occurs quite regularly along the spherulite radii. In such

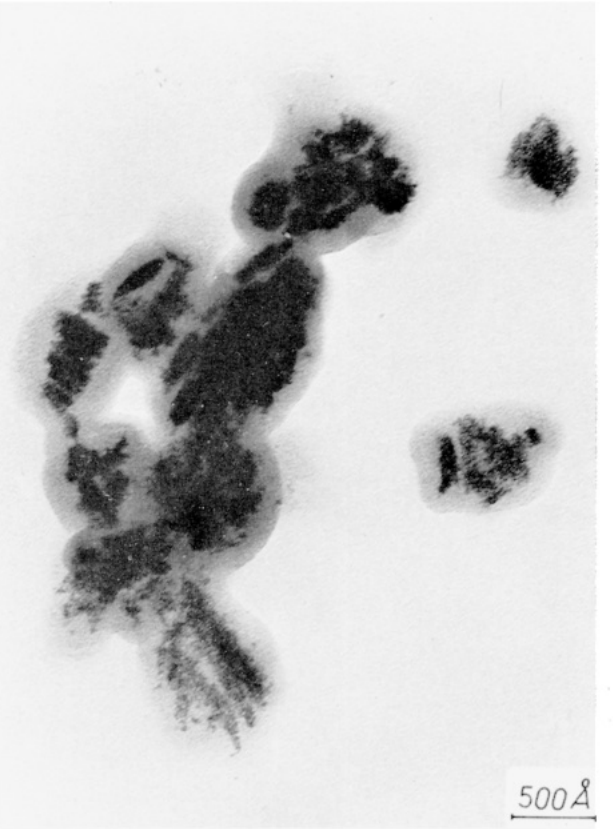

Figure 12. Electron micrograph of deposited sediment from a dissolved nylon 6 sample which had been deformed and infiltrated with OsO_4.

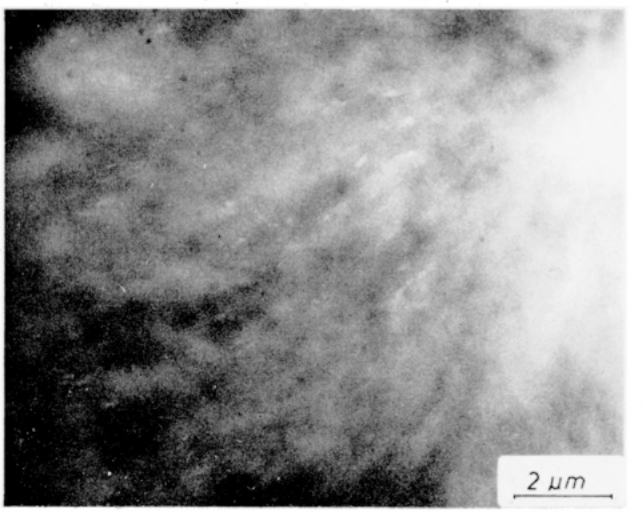

Figure 13. Electron micrograph of a section of deformed dry compression molded nylon 6 etched with sodium metaperiodate.

places, cavitation or other structural damage of the material may be triggered.

These hypotheses are all consistent with the observation that the dark spots are rather small in size, dispersed along radii of spherulites, and split in three to four dark rods. The dark rods could correspond to disrupted interlamellar amorphous layers in a domain which has been subjected to an excessive stress. The last conclusion is supported by the behavior of nylon 6 containing some absorbed water. As already stated above, water acts as a plasticizer of the amorphous phase in nylon 6, decreasing its glass transition temperature, modulus, and yield stress. The plasticized amorphous phase is thus able to undergo large plastic deformation without cavitation. Little or no damage to

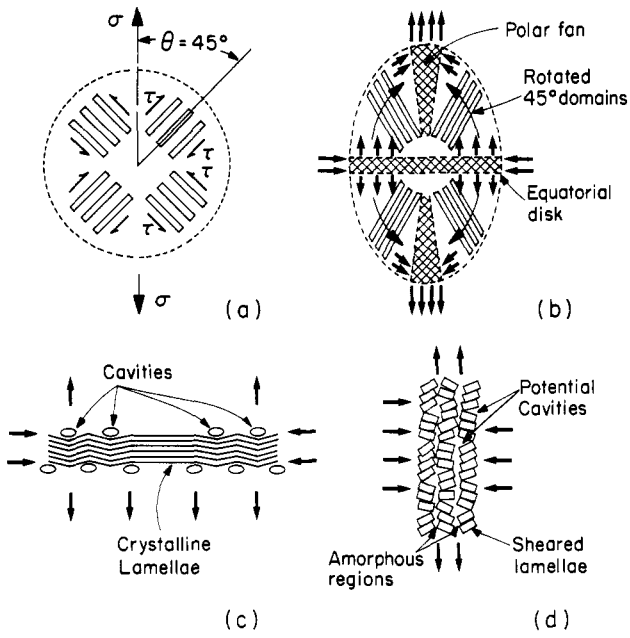

Figure 14. Stages in the formation of cavities in the equatorial regions of spherulites: (a) the 45° domains in an undeformed spherulite; (b) lattice rotations due to simple shear in 45° domains subject equatorial regions to enhanced tension and radial compression and polar regions to enhanced compression; (c) kinking of nondeforming lamellae due to shear instability in the amorphous matrix in equatorial region; (d) shear instability due to chain slip in lamellae in polar regions.

the chemical structure is then caused by the large plastic deformation, and as a consequence, very few dark spots are observed.

Another important observation reported here is that careful examination of ultrathin sections of plastically deformed nylon 6 revealed no regular lamellar structure. This indicates that some drastic rearrangement in crystalline and amorphous phases took place. It also suggests that if the hypotheses offered above are correct, the chemically damaged regions which become dark spots after fixation with OsO_4 are formed during the deformation when the lamellar structure is still pronounced and influences the deformation process. Spherulites should not be expected to survive in plastically deformed nylon 6 bulk samples when draw ratios reach values between 2 and 3. However, a trace of the spherulitic structure is preserved in the form of radially aligned dark spots and radially oriented strips of stronger or weaker stained material—the remnants of radially oriented domains of lamellae. These two features give the impression of the existence of spherulites, although the basic elements of spherulite morphology, the lamellae, are gone.

Better recognition of spherulitic ordering is achieved in the transverse, rather than in longitudinal, sections, because the displacements of crystalline elements during deformation are smaller in that projection and because of radial symmetry the spherulites still have circular outlines. The draw ratio of 2–2.5 for the samples is more or less reflected in the spherulite outlines after deformation.

To our knowledge, there has been no prior direct electron microscopic observation of deformation-induced cavitation or zones of reduced density in nylon 6. Others have postulated that such regions might be produced, on the basis of evidence obtained in light microscopy[26,27] and diffusion experiments.[28] Light microscopy, in particular, supports our present conclusion that the equatorial regions of the spherulites are particularly susceptible to this microvoiding mechanism. Schaper et al.[27] point out that while density decrease and microvoiding appear in the early stages of deformation, peaking around stretch ratios in the region $\lambda = 2$, at higher strains, this void structure disappears, leaving no direct evidence of its previous presence in the deformation process. Their attempts at direct electron microscopic observation of successive stages of deformation were not successful. Therefore, only the final stages ($\lambda = 4$) of disorganized fine structure within the still-visible contours of previously existing spherulites could be studied in detail by them.[27]

In our experiments, we have used materials, specimen geometries, and a form of deformation which led to natural draw ratios in the range of about 2.5, where the microvoiding phenomenon is particularly prevalent. These experimental conditions, coupled with our use of OsO_4 at 4 °C to fix under stress the deformation damage in stretched specimens, made it possible to reveal clearly these deformation-induced damage zones in TEM. We have noted here that stress release and relaxation tend to allow for healing of the microvoids, thereby hiding them from EM observation. We have also recently verified[29] that under certain deformation conditions incorporating pressure, the microvoiding mechanism may be inoperative. Electron micrographs of samples deformed in rolling experiments taken to elongations of $\lambda = 2.5$ revealed a highly oriented texture with no evidence of the black spots shown above. Densities of the rolled samples were higher than those of samples stretched in uniaxial tension to $\lambda = 2.5$, although still somewhat lower than the starting density. In addition, rolled samples are translucent, unlike the opaque starting materials and stretched materials.

In summary, we have presented direct electron microscopic evidence for a mode of deformation of bulk spherulitic nylon 6, which involves chemical damage, cavitation, and/or density reduction in localized regions of the microstructure. This mechanism is difficult to track quantitatively, because high elongations and/or time-dependent healing phenomena tend to mask any direct evidence for its occurrence. Clearly, the mechanism of inhomogeneous deformation discussed above and its associated cavitation phenomenon are sensitive to the macroscopically imposed deformation pattern. Nevertheless, it is clear that any quantitative description of texture evolution in nylon 6 will need to include an appreciation of this important phenomenon of effective reduction of constraints on deformation.

The above conclusions point out that the mechanical properties of amorphous and crystalline phases, however important, are not the only factors influencing the behavior of spherulitic semicrystalline polymers during deformation and that the details of the complex internal structure of spherulites play a decisive role in the mechanism of plastic deformation of bulk nylon 6.

Acknowledgment. This research has been supported by the MRL Division of the National Science Foundation through the Center for Materials Science and Engineering at MIT, under Grant DMR-84-18718. The Fulbright-Hays Program is gratefully acknowledged for providing a Fulbright grant to one of us (A.G.). Partial support of this research was provided by Monsanto Polymer Products Co. of Springfield, Massachusetts. The authors also wish to thank Dr. Carl Dupre of Monsanto for supplying the RIM samples.

Registry No. Nylon 6, 25038-54-4.

References and Notes

(1) Starkweather, H. W.; Moore, G. E.; Hansen, J. E.; Roder, T. M.; Brooks, R. E. *J. Polym. Sci.* **1985**, *21*, 189.

(2) Keith, M. D.; Padden, F. J.; Vadimsky, G. R. *J. Polym. Sci., Polym. Chem. Ed.* **1966**, *A24*, 267.
(3) Keith, M. D.; Padden, F. J. *J. Appl. Phys.* **1964**, *35*, 1270.
(4) Price, F. P.; Kilb, R. W. *J. Polym. Sci., Polym. Phys. Ed.* **1962**, *57*, 395.
(5) Hay, I. R.; Keller, A. *Kolloid Z., Z. Polym.* **1965**, *204*, 43.
(6) Samuels, R. J. *J. Macromol. Sci., Phys.* **1970**, *B4*, 701.
(7) Oda, T.; Nomura, S.; Kawai, H. *J. Polym. Sci.* **1965**, *A3*, 1943.
(8) O'Leary, K. J.; Geil, P. H. *J. Macromol. Sci., Phys.* **1962**, *B2*, 261.
(9) Bessel, T. J.; Hull, D.; Shortall, J. B. *J. Mater. Sci.* **1975**, *10*, 1127.
(10) Shultz, J. M. *Polym. Eng. Sci.* **1984**, *24*, 770.
(11) Galeski, A.; Piorkowska, E. *J. Polym. Sci.* **1983**, *21*, 1299.
(12) Peterlin, A. *Colloid Polym. Sci.* **1975**, *253*, 809.
(13) Peterlin, A. In *Polymeric Materials*; Baer, E., Ed.; American Society for Metals: Metals Park, OH, 1975; p 175.
(14) Gabbert, J. D.; Garner, A. Y.; Hedrick, R. M. Presented at SAE International Congress & Exposition, Detroit, MI, Feb 1982; SAE Technical Paper Series 820420.
(15) Galeski, A.; Argon, A. S.; Cohen, R. E. *Makromol. Chem.* **1987**, *188*, 1195.
(16) Schaper, A.; Hirte, R.; Ruscher, C.; Hillebrand, R.; Walenta, E. *Colloid Polym. Sci.* **1986**, *264*, 649.
(17) Gurato, G.; Fichera, A.; Grandi, F. Z.; Zanetti, R.; Canal, P. *Makromol. Chem.* **1974**, *175*, 953.
(18) Gebizlioglu, O. S.; Cohen, R. E.; Argon, A. S. *Makromol. Chem.* **1986**, *187*, 431.
(19) Martinez-Salazar, J.; Cannon, C. G. *J. Mater. Sci., Lett.* 1984, *3*, 693.
(20) Peterlin, A. *J. Phys. Chem.* **1971**, *75*, 3921.
(21) Kambour, R. P. *Macromol. Rev.* **1973**, *7*, 1.
(22) Argon, A. S.; Cohen, R. E.; Gebizlioglu, O. S.; Schwier, E. E. In *Advances in Polymer Science*; Kausch, H. H. Ed.; Springer: Berlin, 1983; Vol. 52–53, p. 275.
(23) Kramer, E. J. In *Advances in Polymer Science*; Kausch, H. H., Ed.; Springer: Berlin, 1983; Vol. 52–53, p. 1.
(24) Argon, A. S. In *Treatise on Materials Science and Technology*; Herman, H., Ed.; Academic: New York, 1972; Vol. 1, p 79.
(25) Galeski, A.; Koenczoel, L.; Piorkowska, E.; Baer, E. *Nature (London)* **1987**, *325*, 40.
(26) Weynant, E.; Haudin, J. M.; G'Sell, C. *J. Mater. Sci.* **1980**, *15*, 2677.
(27) Schaper, A.; Hirte, R.; Ruscher, C. *Colloid Polym. Sci.* **1986**, *264*, 668.
(28) Peterlin, A. *J. Macromol. Sci., Phys.* **1975**, *B11*, 57.
(29) Gebizlioglu, O. S.; Argon, A. S.; Cohen, R. E., submitted for publication.

Effects of Thermal History on Crystallization of Poly(ether ether ketone) (PEEK)

Youngchul Lee* and Roger S. Porter

Polymer Science and Engineering Department, University of Massachusetts, Amherst, Massachusetts 01003. *Received October 22, 1987; Revised Manuscript Received March 29, 1988*

ABSTRACT: The crystallization of poly(ether ether ketone) (PEEK) has been investigated as a function of thermal history. Isothermal (315, 311 °C) and nonisothermal crystallizations of two reactor powders and one film have been conducted by differential scanning calorimetry (DSC). Isothermal crystallizations at 315 °C have been analyzed by using the Avrami equation. As the temperature in the melt was increased, the Avrami exponent (n) slightly increased (from 3.4 to 3.8), but the parameter k decreased and the crystallization exotherms on cooling (−10 °C/min) shifted to lower temperatures. As the holding time in the melt was increased, the isothermal crystallization curves shifted to longer time. These observations are consistent with a persistence of small residual crystalline regions in the bulk. When the melt of PEEK has been held at or above 390 °C, the subsequent crystallization behavior (isothermal as well as nonisothermal) is nearly independent of the prior melt temperature. It is thus proposed that the residual crystalline regions only persist up to the thermodynamic melting point. Several semicrystalline polymers, including PEEK, support this description. The thermal stability at the melt temperatures has been assessed by thermogravimetric analysis (TGA) and by solution viscosity.

Introduction

Considerable attention has been given to poly(ether ether ketone) (PEEK) as a high performance thermoplastic, as well as a matrix for advanced composites.[1-5] The repeat unit of PEEK is

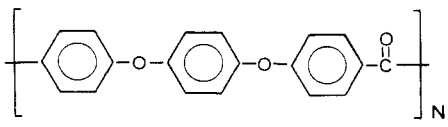

Its glass transition temperature (T_g) is ~143 °C, its common melting temperature ~334 °C, and its crystallinity is 0–48%, depending on sample history.[6] Alterations in crystallization conditions are known to result in different crystal morphologies, which influence product properties.

* Current address: Textile Processing Laboratory, University of Tennessee, Knoxville, TN 37996.

It has been known that the thermal history in the melt or solution affects the crystallization behavior of many polymers.[7] Therefore, the thermal history prior to crystallization must be treated carefully, as well as other crystallization conditions. As the melt temperature is increased, the number of nuclei decreases and, therefore, overall crystallization rate decreases. Reported examples are polyethylene,[8] isotactic polypropylene,[9] isotactic polystyrene,[10] poly(chlorotrifluoroethylene),[11,12] nylon 6,[13] nylon 6,6,[14] poly(ethylene oxide),[15,16] poly(oxymethylene),[17] and poly(ethylene terephthalate).[18,19] Unlike solution crystallization,[20,21] the holding time in the melt also influences the crystallization of polymers.[13,14,17] However, contradictory results have been also obtained for polyethylene[22] and poly(decamethylene terephthalate);[23] crystallizations of the polymers were found to be independent of the previous melt temperature.

It has been noted that crystallization of PEEK in composites depends on melt temperature (melt-annealing temperature) and holding time in the melt (melt-annealing

0024-9297/88/2221-2770$01.50/0